

# Enhanced metabolism of LDL aggregates mediated by specific human monocyte IgG Fc receptors

Peter M. Morganelli,<sup>1</sup> Rick A. Rogers,<sup>2</sup> Tamar J. Kitzmiller, and Alan Bergeron

Veteran's Administration Hospital, White River Junction, VT 05009, and Department of Microbiology, Dartmouth Medical School, Hanover, NH 03755

**Abstract** Macrophage-derived foam cells are important constituents of atheromatous lesions. In addition to the scavenger receptor pathway, uptake of immune complexed lipoproteins through IgG Fc receptors (Fc $\gamma$  receptors) represents an additional pathway of macrophage foam cell development that may be important during atherogenesis. The importance of this mechanism is suggested by studies showing that the titer of autoantibodies to modified lipoproteins correlated with the extent of occlusive disease in patients, and that those antibodies exist in human lesions. Human mononuclear phagocytes possess three structurally and functionally distinct classes of Fc $\gamma$  receptors, each of which could be associated with a unique pathway of lipoprotein metabolism. In order to determine whether uptake of an acute lipid load through each type of Fc $\gamma$  receptor was associated with foam cell development, we used bispecific antibodies consisting of anti-LDL monoclonal antibodies conjugated to anti-Fc $\gamma$  receptor monoclonal antibodies to study the effects of targeting LDL aggregates to each specific type of Fc $\gamma$  receptor on freshly isolated adherent human monocytes. Relative to appropriate controls, LDL degradation, cellular sterol mass, and foam cell development of monocytes were enhanced by targeting LDL aggregates to Fc $\gamma$ RI or Fc $\gamma$ RII, and this was accompanied by an apparent impairment of LDL degradation. Uptake was specific to the Fc $\gamma$  receptors and was not influenced by the presence of scavenger receptor ligands. Thus, with the bispecific approach, the functions of each class of Fc $\gamma$  receptor can be studied on an individual basis with respect to several aspects of cellular cholesterol metabolism. This will be critical for determining which of these receptors are potentially most important in the clearance of lipoprotein immune complexes during atherogenesis.—**Morganelli, P. M., R. A. Rogers, T. J. Kitzmiller, and A. Bergeron.** Enhanced metabolism of LDL aggregates mediated by specific human monocyte IgG Fc receptors. *J. Lipid Res.* 1995. **36**: 714–724.

**Supplementary key words** Fc receptors • monocytes • lipoproteins • immune complexes • bispecific antibodies

Macrophage-derived foam cells are important constituents of atheromatous lesions, contributing in several ways to the intimal inflammation characteristic of lesion development (1, 2). Several mechanisms have been proposed concerning foam cell development in vivo, derived from in vitro studies of lipid-loading with rodent peritoneal macrophages or human peripheral blood

mononuclear phagocytes (reviewed in ref. 3). While much evidence suggests that native LDL does not undergo significant uptake by most types of macrophages in vitro or in vivo (3), uptake of chemically modified LDLs such as acetylated or oxidized LDL by macrophage scavenger receptors results in foam cell development in vitro (3, 4). In addition to scavenger receptors, uptake of immune complexed lipoproteins through IgG Fc receptors (Fc $\gamma$ R) represents another potential mechanism of foam cell development that may also contribute to atherosclerosis, as shown in both mouse peritoneal (5, 6) and human monocyte-derived macrophages (7, 8). The importance of these findings is underscored by the fact that serum autoantibodies to lipoproteins such as oxidized LDL exist in numerous situations clinically, often associated with abnormalities of lipid metabolism including enhanced atherosclerosis (9–12). Recently it was demonstrated that the titer of autoantibodies to oxidized LDL correlated with the extent of carotid disease in Finnish men (12), and antibodies specific to epitopes of oxidized LDL were subsequently detected in human atheromatous lesions (13). These results suggest that the clearance of lipoprotein immune complexes by macrophage Fc $\gamma$ R contributes to foam cell development in vivo. In comparison to other mechanisms of foam cell development, this mechanism has received relatively little attention.

Human mononuclear phagocytes possess three structurally and functionally distinct classes of Fc $\gamma$ R (Fc $\gamma$ RI, Fc $\gamma$ RII, and Fc $\gamma$ RIII) (reviewed in refs. 14, 15), with two or more genetic isoforms in each class, some of which

Abbreviations: BsAb, bispecific antibody; Fc $\gamma$  R, IgG Fc receptor; Ig, immunoglobulin; mAb, monoclonal antibody; LDL-IC, low density lipoprotein immune complexes; LPDS, lipoprotein-deficient serum; vxLDL, vortex-aggregated low density lipoprotein; M $\phi$ , monocyte; HPLC, high performance liquid chromatography.

<sup>1</sup>To whom correspondence should be addressed at: Research 151, Veteran's Administration Hospital, White River Junction, VT 05009.

<sup>2</sup>Current address: Physiology Program, Department of Environmental Health, Harvard School of Public Health, 665 Huntington Avenue, Boston, MA 02115.

define functional differences (15). Fc $\gamma$ R I is the receptor of monocytes and macrophages that binds monomeric human IgG with high affinity (16). Fc $\gamma$ R II and Fc $\gamma$ R III are low affinity receptors that do not bind monomeric IgG but react with particular types of IgG immune complexes with high affinity (17, 18), and are present on monocytes and macrophages as well as on granulocytes and natural killer cells. Fc $\gamma$ R II is also present on platelets and B lymphocytes. While others have shown that uptake of generic lipoprotein immune complexes via macrophage Fc $\gamma$ R results in foam cell development (5–8), the metabolism of lipoproteins after uptake via specific classes of Fc $\gamma$ R has not been studied. This is an important point as each class of Fc $\gamma$ R could be associated with a unique pathway of lipoprotein metabolism. As generic IgG-containing immune complexes prepared with human, rabbit, or murine IgG isotypes could react simultaneously to each type of Fc $\gamma$ R (14, 15, 19, 20), we developed a model to study LDL uptake and cholesterol metabolism in association with each specific class of Fc $\gamma$ R (21). This model is based on the use of bispecific antibodies (BsAb) consisting of apolipoprotein B-specific monoclonal antibodies (mAb) conjugated to anti-Fc $\gamma$ R mAb that are specific for and that trigger function of each of the different types of Fc $\gamma$ R (14). Thus, in the presence of LDL, bispecific LDL immune complexes (LDL-IC) form that will interact with a specific type of Fc $\gamma$ R, e.g., Fc $\gamma$ R I, Fc $\gamma$ R II, or Fc $\gamma$ R III, via anti-Fc $\gamma$ R specific Fab regions. This approach is physiologically relevant because similar to endogenous immune complexes, bispecific immune complexes elicit Fc $\gamma$ R specific functions through receptor cross-linking (14, 15). The results of our previous studies indicated that soluble bispecific LDL-IC targeted to Fc $\gamma$ R of human monocytes underwent cellular internalization and degradation independently of native LDL and scavenger receptors (21), and suggested that BsAb would be important tools for the study of the effects of LDL metabolism in conjunction with specific Fc $\gamma$ R. As one of our goals is to determine whether uptake of LDL-IC by each type of Fc $\gamma$ R or other cell surface molecules is associated with foam cell development, in the present study we used LDL-IC prepared by opsonizing vortex-aggregated LDL (vxLDL) with bispecific anti-Fc $\gamma$ R  $\times$  anti-LDL antibodies to study the effects of acute lipid loading in conjunction with specific Fc $\gamma$ R of human monocytes. Monocytes are important in atherogenesis not only because they represent the origin of intimal macrophages, but also because they are a component of fatty streaks of early lesions (22). As scavenger receptor activity on freshly isolated monocytes is low (23, 24), uptake of immune complexed lipoproteins by monocyte Fc $\gamma$ R could represent an important pathway of foam cell development, especially in the case of aggregated lipoproteins, which may exist in aortic intima in vivo (25). In previous studies, treatment of mouse peritoneal (26) or human monocyte-derived mac-

rophages (27) with aggregated LDL resulted in enhanced uptake and degradation relative to that of native LDL, with a concomitant increase in cellular sterol content and foam cell development. This effect was mediated by the receptor for native LDL, but as shown by Khoo et al. (6) uptake of aggregated LDL by mouse peritoneal macrophages was enhanced in the presence of apolipoprotein B-specific mAb by uptake via Fc $\gamma$ R. Here we report the results of targeting LDL aggregates to Fc $\gamma$ R I or Fc $\gamma$ R II of adherent human monocytes in vitro, which are the major types of Fc $\gamma$ R at that stage of differentiation. We determined that uptake and metabolism of LDL aggregates were enhanced by targeting to these two specific classes of Fc $\gamma$ R. This was accompanied by increases in both cellular sterol mass and extent of foam cell development. Thus, these data suggest that both types of Fc $\gamma$ R may be important in clearance of LDL-IC and foam cell development during atherogenesis.

## MATERIALS AND METHODS

### Miscellaneous reagents

Sterol standards were obtained from Sigma Chemical Company. Na<sup>125</sup>I was obtained from Amersham. All solvents used were of HPLC grade and were obtained from Fisher Scientific. Unless otherwise indicated, all other chemicals or reagents were obtained locally or from Sigma. Lipoprotein-deficient serum (LPDS) was prepared from fetal bovine serum (Hyclone) by ultracentrifugation according to standard techniques (28).

### Antibody preparations

All mAb used were of murine origin. Purified intact or Fab<sub>2</sub> or Fab fragments of anti-Fc $\gamma$ R I (mAb 22, an IgG1) and anti-Fc $\gamma$ R II (mAb IV.3, an IgG2b) were obtained from Medarex, Inc., Annandale, NJ. Anti-Fc $\gamma$ R I mAb 22 binds to an epitope of Fc $\gamma$ R I that is distinct from the ligand binding site; thus its binding is unaffected by the presence of human IgG (16). Anti-Fc $\gamma$ R II mAb IV.3 binds to the ligand binding site of Fc $\gamma$ R II (17). Anti-LDL mAb A01609, which was used in our previous study, is a high affinity apoB-specific IgG1 that was obtained in purified form from Medix Biotech Inc., Foster City, CA. Anti-LDL-1 is an IgG1 that effectively cross-competes with A01609 for binding to native LDL (not shown) and was used as the anti-LDL parent for production of BsAb. This mAb was prepared according to standard techniques (29) by fusing NS-1 nonsecreting myeloma cells (ATCC, Rockville, MD) to splenocytes taken from a mouse immunized with native human LDL. Hybrids were screened for binding to adsorbed native LDL under antioxidant conditions by ELISA (30). The anti-LDL-1 clone was isolated by limiting dilution, expanded in serum-free Excel medium (JRH Scientific, Lenexa, KS) in a hollow-fiber

cartridge (Amicon) and mAb was purified from concentrated supernatants on an ABx ion exchange column (JT Baker). Fab'<sub>2</sub> fragments of anti-LDL-1 were prepared by pepsin digestion with a kit purchased from Unisyn Technologies (Tustin, CA) that included a Protein-A column to remove intact immunoglobulin (Ig). All Fab'<sub>2</sub> preparations were verified to contain negligible amounts of intact Ig by SDS polyacrylamide gel electrophoresis and silver staining and/or analytical HPLC sieving (not shown). BsAb were prepared by chemically conjugating intact or Fab'<sub>2</sub> fragments of anti-FcγRI or anti-FcγRII to intact or Fab'<sub>2</sub> fragments of anti-LDL-1 with *N*-succinimidyl-3-(2-pyridyldithio)propionate (SPDP) and *N*-succinimidyl-S-acetylthioacetate (SATA) as described previously (21). All anti-FcγRI × anti-LDL bispecifics used in this study were prepared with Fab'<sub>2</sub> fragments of both parent mAb. Anti-FcγRII × anti-LDL was prepared with intact mAb.

### Lipoproteins

LDL ( $d > 1.019 < 1.063$  g/ml) was isolated from the serum of fasted donors by ultracentrifugation according to standard techniques and used within 3 weeks (28). Protein content was determined by a modified Lowry assay using bovine serum albumin (BSA) as the standard (31). LDL was labeled with <sup>125</sup>I according to the McFarlane method as described (28). The specific activity of all preparations ranged from 200 to 300 cpm per ng protein, and greater than 98% was acid-precipitable for each preparation. Vortex-aggregated LDL (vxLDL) was prepared according to Khoo et al. (26) by adjusting LDL to 0.5 mg/ml in phosphate-buffered saline (PBS) or serum-free medium in a 15-ml polypropylene tube and vortexing it on a standard laboratory vortexer on high for 60 sec. Acetyl-LDL was prepared according to standard procedures (32). Two preparations were used in these studies; both exhibited the characteristic increase in mobility in 0.5% agarose gels (not shown).

### mAb binding to vxLDL

The reactivity of antibodies to vxLDL was checked by an indirect immunofluorescence assay similar to one that we used previously to study mAb binding to cells (33). Aliquots of vxLDL (0.15 mg) were added to anti-LDL mAb or BsAb in PBS containing 2 mg/ml BSA (PBS-BSA) in 96-well flat-bottomed microtiter plates for 2 h on ice. Isotype-matched negative controls were included in all experiments. The aggregates were washed three times in ice-cold PBS-BSA, pelleted in the microtiter plate at 1800 *g* for 5 min, and then stained in a second step with FITC-conjugated goat anti-mouse Ig for 1 h on ice (Caltag). They were washed again and fixed with 3% methanol-free formaldehyde (Eastman-Kodak, Rochester, NY) in PBS. Samples were analyzed for green fluorescence on an FACScan (Becton-Dickinson). The excitation wavelength was 488 nm and emission at 515 nm was ana-

lyzed. Particles of vxLDL were gated on the basis of blue forward versus right angle light scatter. Data are expressed as mean fluorescence intensity per aggregate.

### Preparation of monocytes (MØ)

Freshly isolated adherent monocytes were studied in each experiment. MØ were obtained from leukapheresis packs of normal donors as described previously (21, 34). Final preparations typically were greater than 90% MØ as judged by morphology of Wright's stained cytopsin preparations. Viability was assessed by trypan blue exclusion and was always greater than 98%. For each experiment, cells were resuspended in serum-free DMEM (Gibco) containing 25 mM *N*-hydroxyethylpiperazine-*N'*-2 ethanesulfonic acid (HEPES) and 25 µg/ml gentamicin (MØ culture medium), at  $1-2 \times 10^6$ /ml, and 1-2 ml was seeded per well into Costar 24- or 12-well plates, respectively. For confocal microscopy, cells were seeded into 24-well plates containing 12-mm diameter #1 coverslips (Fisher). Cells were incubated for 1-2 h at 37°C and 10% CO<sub>2</sub> to allow adherence; the medium was then removed and the wells received <sup>125</sup>I-labeled or unlabeled LDL-IC in medium containing 5 mg/ml LPDS.

### Preparation of LDL-IC and assay of LDL degradation

LDL-IC was prepared by incubating vxLDL at 0.5 mg/ml with anti-LDL mAb or BsAb for a minimum of 2 h at 4°C. Unless otherwise indicated, unlabeled or <sup>125</sup>I-labeled vxLDL were opsonized with 12.5-25 µg/ml of antibody, diluted to 50 µg/ml based on LDL protein in MØ culture medium containing 5 mg/ml LPDS, and added to adherent cells in 12- or 24-well plates (1 or 0.5 ml per well, respectively). The cells were incubated at 37°C and 10% CO<sub>2</sub> for the times indicated in the text. Degradation of <sup>125</sup>I-labeled LDL was done by assay of acid-soluble products that did not contain free iodide (35). All data were corrected for background degradation by subtracting the value of LDL degradation in the absence of cells. After removing supernatants for assay of acid-soluble products, in some experiments each well was washed twice in 1 ml of ice-cold RPMI 1640 containing 2 mg/ml BSA, then once in serum-free medium. The cells were trypsinized with trypsin (Sigma# T5650, supplemented with 25 mM HEPES, pH 7.4), for 10 min at 37°C. Preliminary experiments were done (not shown) to establish that greater than 96% of the cell-associated radioactivity was removed under these conditions. After trypsin treatment the cells were washed again, then lysed in 0.2 N NaOH, and counted for cell-associated (internalized) radioactivity. Extra wells corresponding to each fraction (degradation or cell-associated) were included for the determination of respective cell proteins by Lowry assay (31). The results of degradation assays are expressed as µg or ng of <sup>125</sup>I-labeled LDL degraded per mg cell protein per time of incubation at 37°C as indicated. The percent

internalized LDL that was degraded was calculated by dividing the sum of degraded plus cell-associated LDL into the amount of degraded LDL and multiplying the quotient by 100.

### Confocal microscopy

For analysis of cells by confocal microscopy, monocytes treated with LDL-IC on coverslips were washed, then fixed in 3% methanol-free paraformaldehyde in PBS. Just prior to analysis each well was stained for 10 min at room temperature with 100 ng/ml of Nile Red in PBS (36), then analyzed with a Sarastro 2000 laser scanning confocal microscope (Molecular Dynamics, Sunnyvale, CA) fitted with an argon-ion laser. Random fields were brought into focus using epifluorescent light so as not to bias for fluorescence. Each field was scanned using a  $100 \times$  (1.4 numerical aperture) objective. The operating conditions of the microscope were set to a laser power of 21.0 mW, and the optical path was adjusted for 488 nm (excitation), and  $> 510$  nm (emission). Images were collected using a photomultiplier tube set to 530 volts with a pixel size of  $0.2 \mu\text{M}$ . Dual scan anaglyph images were examined and the number of lipid droplets per cell was counted.

### Assay of sterol mass

Cellular mass of free and esterified cholesterol was determined by assay of lipid extracts by reversed phase HPLC as described (37, 38). An analytical  $4.6 \times 250$  mm C18 Microsorb column (Rainin Instrument Co., Woburn,

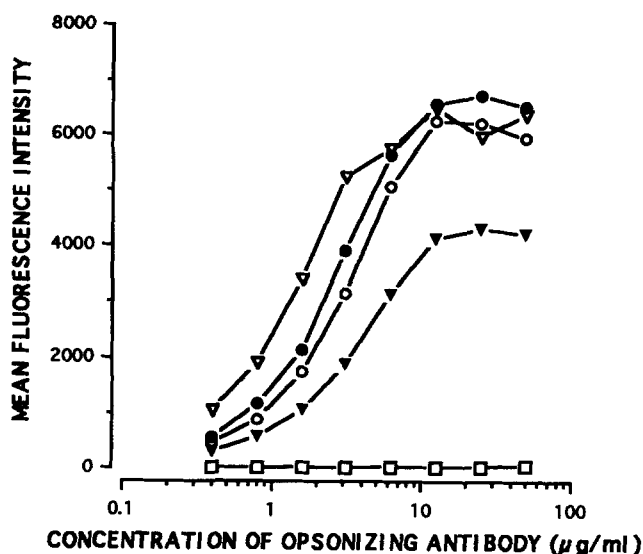


**Fig. 1.** Line plot of the binding of various antibody preparations to LDL aggregates. Suspensions of vxLDL aggregates were stained on ice with varying amounts of anti-LDL mAb or bispecific antibodies, and binding was detected with FITC-conjugated goat anti-mouse Ig and flow cytometric analysis of fixed aggregates. Binding is expressed as the mean fluorescence intensity per aggregate. Open squares, IgG1 control; closed triangles, anti-LDL Fab'2; open circles, anti-Fc $\gamma$ RI  $\times$  anti-LDL; closed circles, anti-Fc $\gamma$ RII  $\times$  anti-LDL; open triangles, anti-LDL IgG1.

MA) with  $5 \mu\text{M}$  bead diameter and  $100 \text{ \AA}$  pore size was used. The mobile phase consisted of acetonitrile-2-propanol 1:1 and absorption at 210 nm was monitored at room temperature of  $22^\circ\text{C}$ . Standard curves were constructed by plotting peak area versus mass of the following sterol standards dissolved in 2-propanol: cholesterol, cholesteryl arachidonate, cholesteryl linoleate, cholesteryl oleate, cholesteryl palmitate, cholesteryl stearate, and cholesteryl heptadecanoate. The latter ester, which does not occur in cells, was used as an internal standard and was added to cell pellets prior to extraction to adjust for procedural losses. The mass/peak area was constant for each sterol, and regression coefficients greater than 0.998 were typically obtained for each standard (not shown). Cells treated with bispecific LDL-IC were washed and trypsinized as described above to remove bound complexes and extracted into chloroform-methanol (39). The extracts were dried under  $\text{N}_2$ , heated for 30 min at  $100^\circ\text{C}$  to remove trace amounts of chloroform, and resolubilized in 2-propanol just prior to analysis. The mass of duplicate samples is expressed as  $\mu\text{g}$  sterol/mg cell protein.

## RESULTS

### BsAb reactivity to vxLDL and degradation of bispecific LDL-IC

**Figure 1** shows antibody binding to vxLDL for each of the different BsAb or anti-LDL preparations used for these studies. As determined by the flow cytometric assay, each antibody preparation demonstrated saturable binding at  $12.5 \mu\text{g/ml}$  of opsonizing antibody. Binding was specific, as there was no reactivity of equivalent amounts of a nonspecific IgG1 isotype control; other irrelevant murine IgG isotypes behaved similarly (not shown). **Figure 2A** shows an experiment where LDL-IC were prepared by opsonizing  $^{125}\text{I}$ -labeled vxLDL with the same concentrations of anti-LDL Fab'2, anti-Fc $\gamma$ RI  $\times$  anti-LDL, or anti-Fc $\gamma$ RII  $\times$  anti-LDL used in the experiment of Fig. 1. The LDL-IC were incubated with freshly prepared and adherent monocytes for 20 h at  $37^\circ\text{C}$  followed by assay of LDL degradation. For both types of LDL-IC, LDL degradation increased with increasing amounts of opsonizing BsAb, nearing a plateau at maximal opsonization ( $12.5 \mu\text{g/ml}$ ). As expected, there was little change in LDL degradation for the anti-LDL Fab'2 opsonized control. By  $25 \mu\text{g/ml}$  of opsonizing BsAb, degradation mediated through Fc $\gamma$ RI was approximately two times control, and degradation through Fc $\gamma$ RII was approximately three times control. Similar results were obtained in other experiments with different preparations of BsAb (not shown), where maximum degradation occurred between 10 and  $25 \mu\text{g/ml}$  of opsonizing antibody. The amount of LDL-IC used to stimulate cells was titrated in a different experiment (Fig. 2B). Monocytes were incubated for 4 h

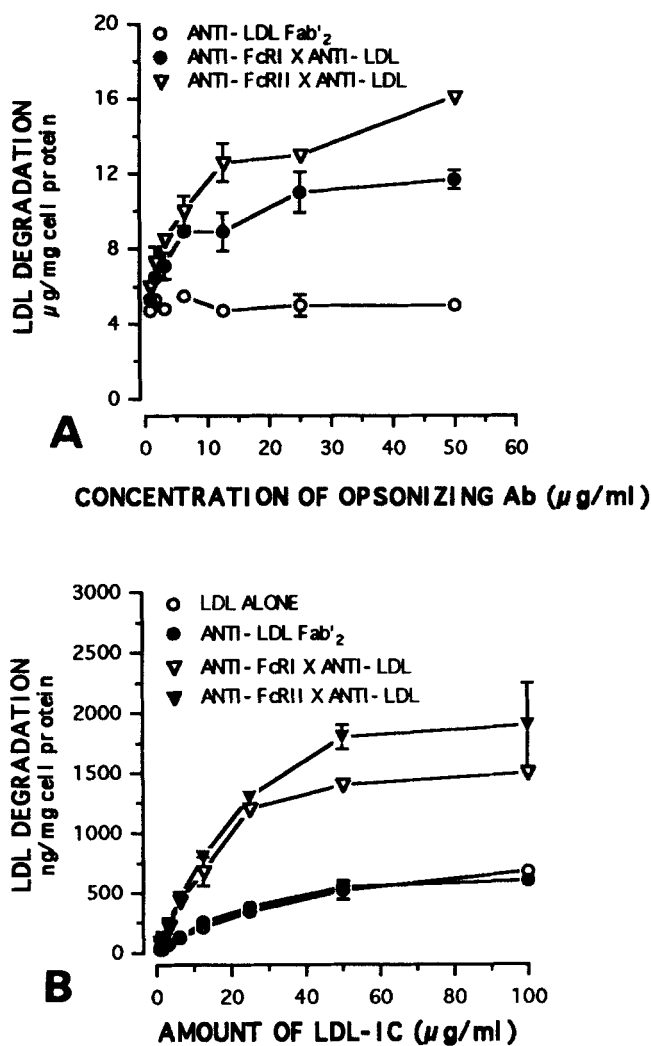


**Fig. 2.** (A) Line plot of the effects of varying degrees of opsonization of LDL aggregates on LDL degradation. Adherent monocytes were treated for 20 h at 37°C with 50  $\mu\text{g/ml}$  of  $^{125}\text{I}$ -labeled vxLDL opsonized with anti-LDL Fab'<sub>2</sub>, and anti-Fc $\gamma$ RI  $\times$  anti-LDL, or anti-Fc $\gamma$ RII  $\times$  anti-LDL. Supernatants were assayed for acid-soluble products that did not contain free iodide. All data were corrected for spontaneous degradation that occurred in the absence of cells. (B) Line plot of LDL degradation after treatment with varying amounts of bispecific LDL-IC. Monocytes were treated with varying amounts of  $^{125}\text{I}$ -labeled vxLDL (based on LDL protein) opsonized with 25  $\mu\text{g/ml}$  of anti-LDL Fab'<sub>2</sub>, anti-Fc $\gamma$ RI  $\times$  anti-LDL, anti-Fc $\gamma$ RII  $\times$  anti-LDL, or no antibody, for 4 h at 37°C followed by assay of LDL degradation. Shown in (A) and (B) are the means  $\pm$  SD of triplicate measurements.

with varying amounts of LDL-IC (based on LDL protein) prepared with either no antibody, anti-LDL Fab'<sub>2</sub>, anti-Fc $\gamma$ RI  $\times$  anti-LDL, or anti-Fc $\gamma$ RII  $\times$  anti-LDL, followed by assay of LDL degradation. In all cases LDL degradation reached a plateau at 50  $\mu\text{g/ml}$  of LDL-IC. Degradation mediated through Fc $\gamma$ RI or Fc $\gamma$ RII was 2.5- and 3.3-times both controls, respectively. There were no differences in degradation between LDL alone and the anti-LDL Fab'<sub>2</sub> control, and this was a consistent result in all experiments that included both of those controls.

Thus, the binding of anti-LDL Fab'<sub>2</sub> to vxLDL did not appear to affect its subsequent uptake and degradation through native LDL receptors or nonspecific pathways. The same results were obtained in a different experiment with cells from a different donor (not shown). Thus, in all subsequent experiments LDL-IC were prepared with 25  $\mu\text{g/ml}$  of antibody and used at 50  $\mu\text{g/ml}$  of LDL protein.

#### Time course studies

In order to determine the point at which uptake of LDL-IC through specific Fc receptors was maximal, several time course studies were done. There were two formats to these studies. For the first studies (Fig. 3), cells were treated for 0–20 h at 37°C in the continuous presence of bispecific  $^{125}\text{I}$ -labeled LDL-IC; in the second series of studies (Fig. 4), cells were pulsed with bispecific LDL-IC for 3 h at 37°C, then washed and chased in 5 mg/ml LPDS in the absence of bispecific  $^{125}\text{I}$ -labeled LDL-IC. In both cases, LDL degradation and internalized but undegraded LDL (referred to as cell-associated LDL) were measured at several time points. **Figure 3 (A)** shows a typical experiment of cells treated in the continuous presence of  $^{125}\text{I}$ -labeled LDL-IC. By 10 h of incubation, degradation of LDL aggregates associated with Fc $\gamma$ RI and Fc $\gamma$ RII was 2- and 3-times that of the anti-LDL Fab'<sub>2</sub> control, respectively. LDL aggregates targeted to Fc $\gamma$ RI or Fc $\gamma$ RII were degraded more rapidly than LDL alone for the first 10 h. From 10 to 20 h, degradation in each case proceeded at a similar rate, but did not level off completely. Plateaus in degradation associated with Fc $\gamma$ RI and Fc $\gamma$ RII were evident, however, when those data were corrected by subtracting the values of the anti-LDL Fab'<sub>2</sub> control (not shown). This is consistent with a nonspecific component of binding and uptake of LDL aggregates as reported by others (40, 41). **Figure 3 (B)** shows the changes in cell associated LDL. For anti-LDL Fab'<sub>2</sub> as well as for each type of bispecific LDL-IC there was a rapid increase in cell associated LDL by 3 h of incubation that exceeded the amount of LDL degradation. By 6 h cell-associated LDL had decreased and then tended to level off, but exceeded degradation at each time point. As this may have been related to an overload of lysosomal compartments because of the continued presence of LDL or LDL-IC, two experiments of the second format were done. **Figure 4** shows the results of LDL degradation and cell-associated LDL in cells pulsed with  $^{125}\text{I}$ -labeled vxLDL or bispecific  $^{125}\text{I}$ -labeled LDL-IC and then chased in the absence of LDL or LDL-IC as described above. The results were similar to those shown in Fig. 3. LDL degradation was significant by 3 h of incubation and increased throughout the chase. While cell-associated LDL (Fig. 4B) did not exceed LDL degradation to the same extent as shown in Fig. 3, there was still incomplete degradation of LDL and LDL-IC by 20 h of incubation. The insets in Figs. 3 and 4 show the data plotted as the percent

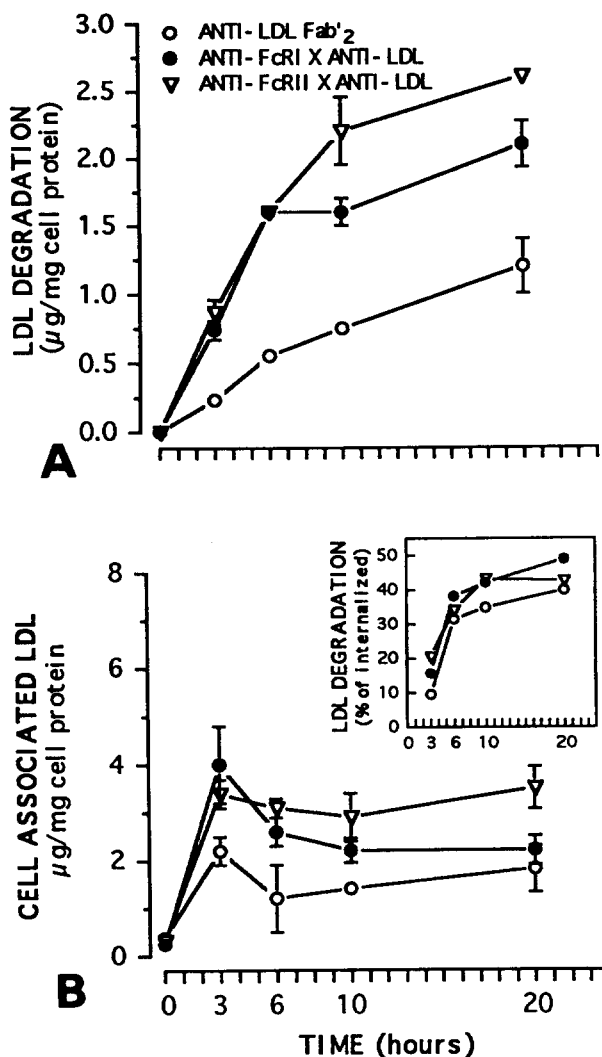


**Fig. 3.** Time course study of the effects of continuous stimulation of adherent monocytes with bispecific LDL-IC. Adherent monocytes were treated at 37°C with 50 µg/ml of <sup>125</sup>I-labeled vxLDL opsonized with 25 µg/ml of anti-LDL Fab'2, anti-FcγRI × anti-LDL, or anti-FcγRII × anti-LDL. (A) At 0, 3, 6, 10, and 20 h of incubation cells were placed on ice and supernatants were assayed for LDL degradation. (B) At each time point cells were washed and treated with trypsin as described in Methods, then lysed and harvested for determination of cell-associated (internalized but undegraded) LDL. The inset shows a line plot of LDL degradation expressed as a percent of total internalized LDL [(degraded/degraded plus cell-associated) × 100]. Shown in (A) and (B) are the means ± SD of triplicate measurements.

of internalized LDL that was degraded (see Methods). In the continuous presence of ligand, the percent of internalized LDL that was degraded was less than 50% after 20 h of incubation in all cases (inset, Fig. 3). For cells pulsed with ligand then chased in its absence, the percent of internalized LDL that was degraded, although greater than that shown in Fig. 3, varied from approximately 60–70% by 20 h of incubation (inset, Fig. 4). Thus, reducing the amount of ligand with the pulse/chase mode resulted in an increase in the amount of internalized LDL that was

degraded. Degradation, however, was still incomplete by 20 h of the chase period. We performed an additional experiment with the pulse/chase mode that carried the chase out to 72 h. The results were similar to those shown in Fig. 4 (not shown). In all cases degradation was approximately 60–70% by 20 h of chase, but did not increase significantly even after an additional 52 h of chase. Thus, it appeared that the metabolism of aggregated LDL and LDL-IC was not only impaired in that experiment but was actually suspended.

#### Effects of chloroquine on LDL degradation

It has been assumed that the degradation of bispecific LDL-IC that occurs following uptake through Fc recep-

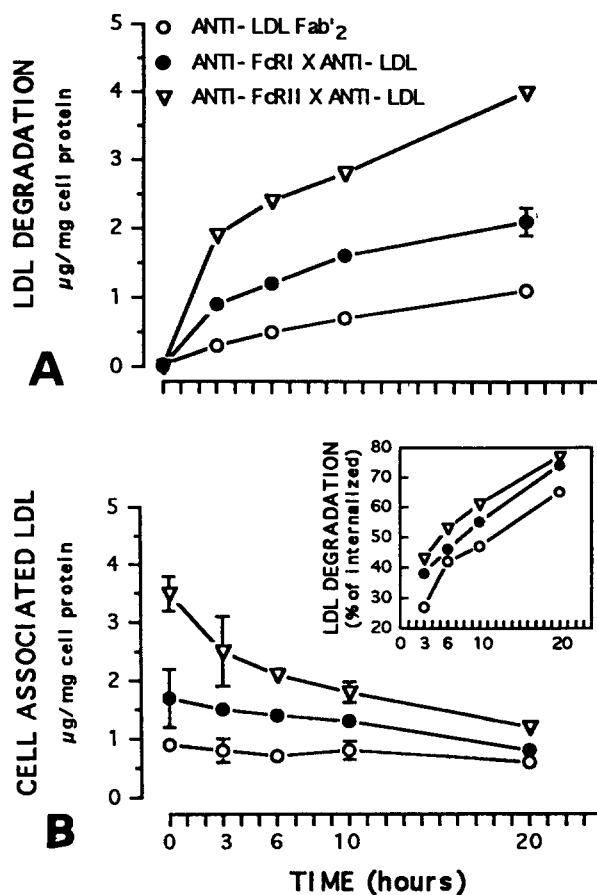


**Fig. 4.** Pulse/chase time course study of LDL degradation after treatment with bispecific LDL-IC. Adherent monocytes were incubated for 3 h at 37°C with 50 µg/ml of <sup>125</sup>I-labeled vxLDL opsonized with 25 µg/ml of anti-LDL Fab'2, anti-FcγRI × anti-LDL, or anti-FcγRII × anti-LDL. After 3 h the cells were washed then chased in 5 mg/ml LPDS. (A) Supernatants were harvested at the indicated time points and assayed for LDL degradation. (B) Cells were treated with trypsin and harvested for determination of cell-associated LDL as described in the legend of Fig. 3. The amount of cell-associated LDL at the zero time point reflects the amount of internalized LDL accumulated during the 3-h pulse. The amount of LDL degradation during the pulse was not determined. The inset shows a line plot of LDL degradation expressed as a percent of total internalized LDL [(degraded/degraded plus cell-associated) × 100]. Shown in (A) and (B) are the means ± SD of triplicate measurements.

tors is the result of lysosomal protease activity following phagocytosis of the LDL-IC. To verify this in our model we studied the effects of chloroquine on the degradation of bispecific LDL-IC. Monocytes were treated for 4 h at 37°C with LDL alone, anti-LDL Fab'<sub>2</sub> opsonized LDL, or with bispecific LDL-IC directed to FcγRI or FcγRII, in the presence and absence of 10, 50, or 100 μg/ml of chloroquine. Consistent with previous experiments, there was a 2.6- and 3.9-fold increase in degradation mediated through FcγRI and FcγRII, respectively, relative to the control. In each case there was at least a 70% decrease in LDL degradation with 100 μg/ml of chloroquine (100 to 30 ng/mg cell protein for both controls; 260 to 80 for FcγRI; 390 to 110 for FcγRII). These data are consistent with inhibition of intracellular lysosomal proteolysis of LDL. The same results were obtained in a similar experiment (not shown).

### Specificity of the response to bispecific LDL-IC

The specificity of each type of anti-FcγR BsAb is essential for determining whether cholesterol metabolism varies with uptake through different types of FcγR. Thus, degradation of <sup>125</sup>I-labeled LDL-IC was studied in the presence or absence of excess anti-FcγR parent mAb or human IgG to establish specificity of each type of bispecific LDL-IC. **Figure 5** shows an experiment where monocytes were treated for 20 h at 37°C with LDL-IC prepared with anti-LDL Fab'<sub>2</sub>, anti-FcγRI × anti-LDL, or anti-FcγRII × anti-LDL, in the presence and absence of excess (50 μg/ml) anti-FcγRI Fab'<sub>2</sub>, anti-FcγRII Fab, or monomeric human IgG (which is a high affinity ligand for

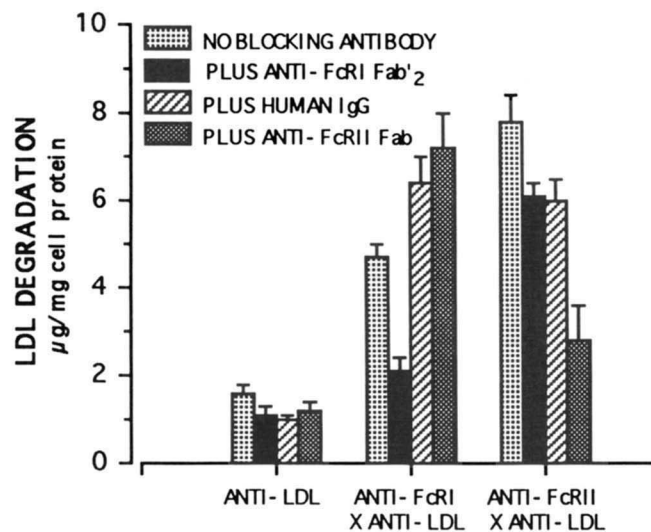


**Fig. 5.** Bar graph demonstrating specificity of the response to bispecific LDL-IC in the presence of FcγR specific ligands. Adherent monocytes were treated for 20 h at 37°C with 50 μg/ml of <sup>125</sup>I-labeled vxLDL opsonized with 25 μg/ml of anti-LDL Fab'<sub>2</sub>, anti-FcγRI × anti-LDL, or anti-FcγRII × anti-LDL, in the presence and absence of 50 μg/ml of anti-FcγRI Fab'<sub>2</sub>, anti-FcγRII Fab, or human IgG. Supernatants were harvested for LDL degradation as described in the legend of Fig. 2. Shown are the means ± SD of triplicate measurements.

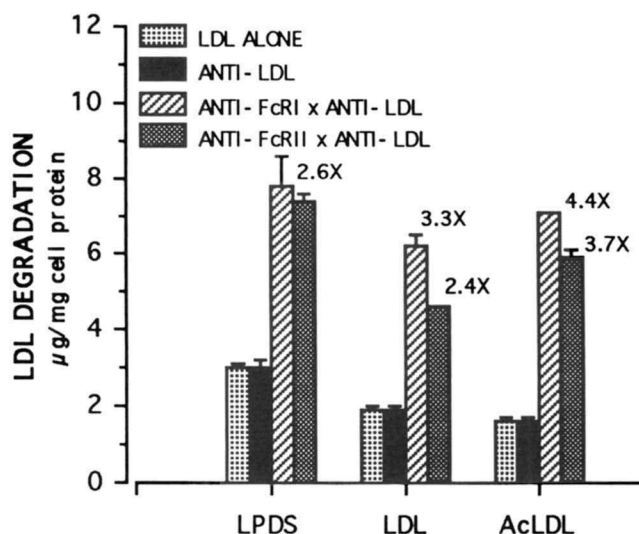


**Fig. 6.** Bar graph demonstrating specificity of the response to bispecific LDL-IC in the presence of LDL receptor or scavenger receptor ligands. Adherent monocytes were treated for 18 h at 37°C with 50 μg/ml of <sup>125</sup>I-labeled vxLDL prepared as described in the legend of Fig. 5, in the presence and absence of 5 mg/ml LPDS, 100 μg/ml of native LDL, or 100 μg/ml of acetyl-LDL. Supernatants were harvested for LDL degradation as described in the legend of Fig. 2. The fold-increases above controls are shown in each case. Shown are the means ± SD of triplicate measurements.

FcγRI; see Antibodies section in Methods for a description of mAb used for these studies). In the absence of blocking antibodies, LDL degradation mediated through FcγRI was greater than 2 times control, and degradation through FcγRII was approximately 3.5 times control. Relative to the anti-LDL Fab'<sub>2</sub> control, LDL degradation through FcγRI was inhibited by 80% in the presence of excess anti-FcγRI mAb indicating that the response was specific to FcγRI. The responses to bispecific FcγRI were slightly enhanced in the presence of excess anti-FcγRII Fab'<sub>2</sub> or human IgG. Enhancement of FcγRI functions in the presence of anti-FcγRII mAb or human IgG have been reported previously (42, 43). Degradation through FcγRII was inhibited by approximately 75% in the presence of anti-FcγRII mAb. Small and identical amounts of inhibition were obtained with monomeric human IgG and anti-FcγRI Fab'<sub>2</sub>, and are not significant because those ligands do not bind to the ligand binding site of FcγRII, which is recognized by the anti-FcγRII BsAb (16).

In three experiments we were not able to obtain complete inhibition of the effects of insoluble LDL-IC with excess soluble anti-FcγR mAb. This was probably due to higher binding avidity of large multimeric insoluble immune complexes in comparison to that of soluble mAb or ligands (44). Thus, we wanted to determine whether some degree of the effects of bispecific LDL-IC were mediated through scavenger receptors. **Figure 6** shows an experiment where monocytes were stimulated at 37°C for 18 h

with bispecific  $^{125}\text{I}$ -labeled LDL-IC in the presence or absence of 100  $\mu\text{g}/\text{ml}$  of either unlabeled native LDL or acetyl-LDL. In the absence of excess lipoproteins (5 mg/ml LPDS) there was approximately a 2.6-fold increase in LDL degradation above controls mediated through  $\text{Fc}\gamma\text{RI}$  or  $\text{Fc}\gamma\text{RII}$ . In the presence of excess native LDL, the increases in degradation were 3.3- and 2.4-fold for  $\text{Fc}\gamma\text{RI}$  and  $\text{Fc}\gamma\text{RII}$ , respectively; in the presence of excess acetyl-LDL, the increases in degradation were 4.4- and 3.7-fold, respectively. The slight decrease in degradation seen for  $\text{Fc}\gamma\text{RII}$  in the presence of excess LDL was probably due to competition between unlabeled and  $^{125}\text{I}$ -labeled LDL for binding to the BsAb. We obtained similar results in uptake studies with fluorophore-conjugated LDL-IC in the presence of excess unlabeled LDL (not shown). As LDL-IC stimulation could potentially trigger the production of superoxide anion that could oxidize LDL causing it to react with scavenger receptors (45), the important point is that the effects of bispecific LDL-IC were not inhibited in the presence of scavenger receptor ligands, and thus the enhancement in degradation mediated by BsAb was specific to Fc receptors.

#### Sterol mass in response to bispecific LDL-IC treatment

It remained to be shown that the enhanced uptake and degradation of bispecific LDL-IC resulted in an increase in cellular sterol mass and foam cell development. Sterol mass was measured in two experiments where monocytes from different donors were treated with unlabeled LDL or bispecific LDL-IC for 24 h at 37°C. The cells were washed and treated with trypsin to remove bound complexes, extracted into chloroform, and analyzed for free cholesterol and cholesteryl ester content as described in Methods. The results are shown in Table 1. In experiment 1, relative to the LDL alone control, there was a 2-fold increase in cholesteryl ester content for LDL uptake through  $\text{Fc}\gamma\text{RI}$ , and a 3-fold increase for uptake through  $\text{Fc}\gamma\text{RII}$ . In experiment 2, there was a 3-fold in-

TABLE 1. Cellular sterol mass in monocytes treated with bispecific LDL-IC

Treatment	Total Sterol	Free Cholesterol	Cholesteryl Esters
Experiment 1			
LDL alone	42.9 $\pm$ 5.2	22.6 $\pm$ 2.2	20.3 $\pm$ 3.0
Anti-FcRI $\times$ anti-LDL	80.1 $\pm$ 9.4	35.7 $\pm$ 1.6	44.4 $\pm$ 8.0
Anti-FcRII $\times$ anti-LDL	95.7 $\pm$ 6.7	35.2 $\pm$ 2.1	60.5 $\pm$ 4.6
Experiment 2			
LDL alone	29.2 $\pm$ 2.2	10.5 $\pm$ 0.9	18.7 $\pm$ 1.3
Anti-FcRI $\times$ anti-LDL	86.2 $\pm$ 3.1	28.0 $\pm$ 0.8	58.2 $\pm$ 2.3
Anti-FcRII $\times$ anti-LDL	51.1 $\pm$ 2.2	16.5 $\pm$ 0.1	34.6 $\pm$ 2.2

Adherent monocytes were treated for 24 h at 37°C with unlabeled aggregated LDL or LDL-IC prepared as described in the legend to Fig. 3. After the incubation, the cells were trypsin-stripped, extracted into chloroform, and analyzed for sterol mass as described in Methods. Values are given as  $\mu\text{g}$  sterol/mg all protein  $\pm$  ranges of duplicate samples.

crease in cholesteryl ester content for uptake through obtained  $\text{Fc}\gamma\text{RI}$ , and a 1.8-fold increase for uptake through  $\text{Fc}\gamma\text{RII}$ . These data suggested that uptake of LDL through  $\text{Fc}\gamma\text{RI}$  or  $\text{Fc}\gamma\text{RII}$  was associated with enhanced foam cell development. To obtain visual confirmation of foam cell development and to determine whether there were differences in the intracellular distribution of lipid in LDL-IC-treated cells, three additional experiments were done. Monocytes adhered to glass coverslips were treated with unlabeled LDL or bispecific LDL-IC for 24 h at 37°C. After incubation they were stained with Nile Red (36) and examined for the presence of intracellular lipid droplets by laser scanning confocal microscopy. Confocal images of the nuclear plane are shown in Fig. 7 for cells from the first experiment. While the greatest number of fluorescent lipid droplets was seen in cells treated with LDL-IC directed to  $\text{Fc}\gamma\text{RI}$  and  $\text{Fc}\gamma\text{RII}$ , in each case the distribution of fluorescence was extensively perinuclear (LDL-alone control, Fig. 7A; anti- $\text{Fc}\gamma\text{RI}$   $\times$  anti-LDL, 7B; anti- $\text{Fc}\gamma\text{RII}$   $\times$  anti-LDL, 7C). Similar results were obtained in two other experiments with different donors (not shown).

#### DISCUSSION

Previously we reported on the effects of targeting soluble LDL to specific  $\text{Fc}\gamma\text{R}$  of human monocytes using bispecific LDL-IC (21). Those studies were concerned primarily with demonstrating the specificity of the bispecific technique, and were done using soluble LDL and nonadherent monocytes under conditions that did not result in lipid loading. The results indicated that targeting native LDL to specific  $\text{Fc}\gamma\text{R}$  resulted in enhanced LDL uptake and degradation that occurred independently of native LDL receptors or scavenger receptors. Those studies established the usefulness of this approach for studying the effects of lipoprotein metabolism associated with specific cell surface molecules, in this case the different types of  $\text{Fc}\gamma\text{R}$ . The present studies were done to determine whether lipid loading of human monocytes through the specific types of  $\text{Fc}\gamma\text{R}$  would enhance foam cell development. We used bispecific antibodies and aggregated LDL to study acute lipid loading of adherent monocytes after uptake through specific  $\text{Fc}\gamma\text{R}$ . LDL degradation, cellular sterol mass, and cellular distribution of neutral lipid were studied for several different donors. Our results confirm and extend those of Khoo et al. (6), who demonstrated enhanced uptake and metabolism of LDL aggregates through  $\text{Fc}\gamma\text{R}$  of murine macrophages in the presence of murine anti-apoprotein B mAb. We determined that targeting LDL aggregates to  $\text{Fc}\gamma\text{RI}$  with bispecific antibodies typically resulted in a 2-fold increase in LDL degradation relative to controls; targeting to  $\text{Fc}\gamma\text{RII}$  typically resulted in a 3- to 4-fold increase in degradation. This difference was observed in uptake and



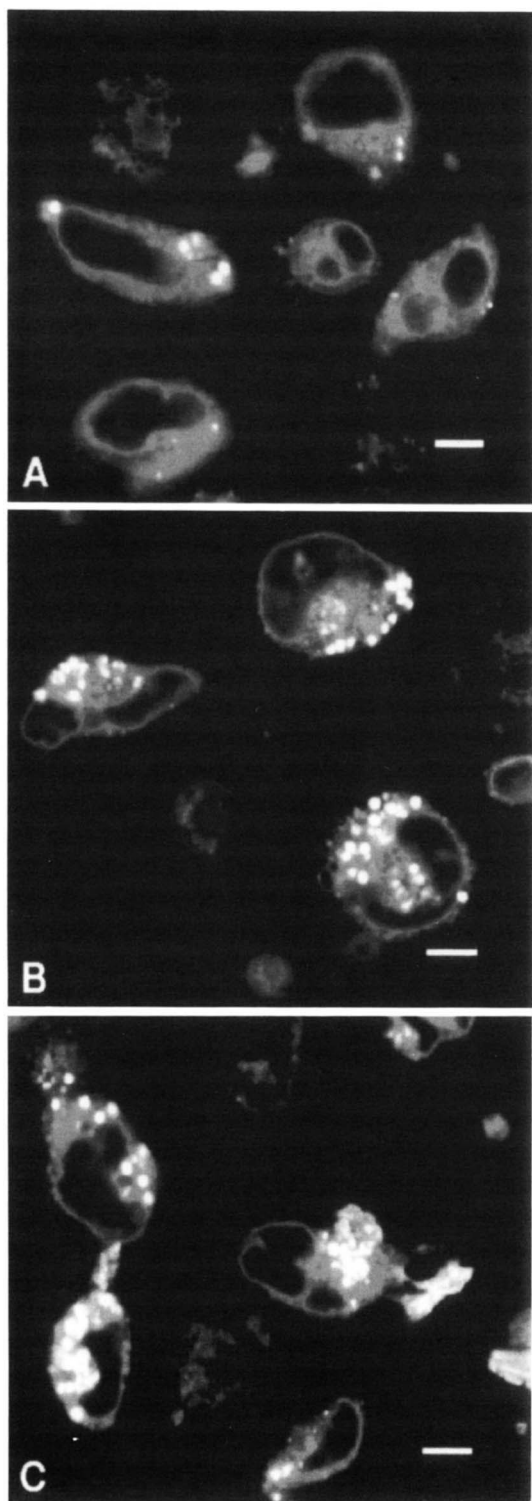


**Fig. 7.** Laser scanning confocal micrograph of neutral lipid droplets in adherent monocytes after treatment with bispecific LDL-IC. Monocytes adhered to coverslips were treated for 24 h at 37°C with 50  $\mu\text{g}/\text{ml}$  of unlabeled vxLDL opsonized with 25  $\mu\text{g}/\text{ml}$  of anti-LDL Fab'2, anti-Fc $\gamma$ RI  $\times$  anti-LDL, or anti-Fc $\gamma$ RII  $\times$  anti-LDL. Coverslips were stained with 100 ng/ml of Nile Red just prior to analysis with a confocal microscope as described in Methods. (A) Cells treated with vxLDL opsonized with anti-LDL Fab'2; (B) with bispecific anti-Fc $\gamma$ RI LDL-IC; (C) with bispecific Fc $\gamma$ RII LDL-IC. Scale bars = 5  $\mu\text{m}$ .

degradation assays in our previous report (21), and in general it appears that more LDL uptake and degradation occurs following targeting to Fc $\gamma$ RII as opposed to Fc $\gamma$ RI (Figs. 2, 3, 4, 5). This may reflect different degrees of expression of the two types of Fc $\gamma$ R. Fc $\gamma$ RII is usually more highly expressed than Fc $\gamma$ RI (14, 15); however, the absolute ranges of expression of Fc $\gamma$ RI and Fc $\gamma$ RII overlap, and it cannot be excluded that the activity of Fc $\gamma$ RII triggered by immune complex ligation is potentially greater than the activity of Fc $\gamma$ RI. It is noteworthy that Fc $\gamma$ RI expression is dramatically increased in response to interferon- $\gamma$  (46). Thus, conditions may exist in vivo where the expression or activity of Fc $\gamma$ RI exceeds that of Fc $\gamma$ RII. The pulse/chase studies (see Results) revealed that degradation was not only impaired after uptake of aggregated LDL via monocyte Fc $\gamma$ R, but was actually suspended beyond 20 h of chase. This was not unique to degradation associated with Fc $\gamma$ R, as the aggregated LDL controls experienced a similar fate. According to Hoff et al. (47), the physical attributes that oxidized LDL acquires by self-aggregation is only partially responsible for the poor intracellular degradation of that lipoprotein in mouse peritoneal macrophages; differences in intracellular trafficking amongst different lipoprotein preparations could also be a contributing factor. Thus, these may be factors in the impaired degradation of LDL and LDL-IC in monocytes of the present studies. Previous studies by Lopes-Virella et al. (8) showed impaired metabolism of insoluble LDL-IC in human macrophages, whereas native soluble LDL was completely degraded under similar conditions. However, in that study the insoluble LDL-IC were nearly completely degraded in a pulse/chase experiment by 28 h of chase. An important difference that could have accounted for their results includes the use of monocyte-derived macrophages that express all three types of Fc $\gamma$ R (14, 15). The freshly prepared and thus less mature monocyte used in our studies may not have had as great a capacity to metabolize immune complexes as does the more mature phenotype.

Table 1 and Fig. 7 show that cellular sterol mass and the extent of foam cell development were enhanced by treating monocytes with bispecific LDL-IC. As shown by Khoo et al. (26), Suits et al. (27), and Heinecke et al. (48), the phagocytosis of native vortex-aggregated or phospholipase C-aggregated LDL resulted in macrophage foam cell development. In our studies the cholesteryl ester content of monocytes treated with bispecific LDL-IC was enhanced approximately 2- to 3-fold relative to the LDL-alone controls. The sterol content of cells treated with LDL aggregates in the absence of BsAb was significant (Table 1), and as expected, some foam cells were observed in response to this treatment by Nile Red staining and analysis of fluorescent neutral lipid droplets (Fig. 7A). However, consistent with the enhancement in LDL degradation and sterol mass that occurred in the presence of

bispecific LDL-IC, there was an enhancement in foam cell development associated with uptake through both types of Fc $\gamma$ R (Figs. 7B and 7C). Differences in the intracellular distribution of lipid droplets were not noted in cells stimulated through Fc $\gamma$ RI or Fc $\gamma$ RII. Because of confocal optics, the images shown in Fig. 7 represent fluorescence confined to a narrowly defined plane of focus, in this case the nuclear plane. Fluorescence that exists above or below the plane of focus is optically excluded. This represents a major advantage over conventional epifluorescence microscopy for analysis of foam cells where fluorescence generated above and below the plane of focus, such as on the cell surface, will usually obscure analysis of intracellular fluorescence.

In summary, we used a novel approach to study the effects of uptake of LDL aggregates in the context of specific Fc $\gamma$ R of adherent human monocytes. LDL degradation, cellular sterol mass, and foam cell development of monocytes were enhanced by targeting LDL aggregates to Fc $\gamma$ RI or Fc $\gamma$ RII. With the bispecific approach the functions of each class of Fc $\gamma$ R can be studied with respect to other aspects of cellular cholesterol metabolism to determine which of these pathways are most important in the clearance of lipoprotein immune complexes and foam cell development in vivo. ■

This work was supported by funds from a Merit Review Award to P. M. M. from the U.S. Department of Veteran's Affairs.

Manuscript received 7 July 1994 and in revised form 23 September 1994.

## REFERENCES

- Ross, R. 1986. The pathogenesis of atherosclerosis — an update. *N. Engl. J. Med.* **314**: 488–500.
- Munro, J. M., and R. S. Cotran. 1988. The pathogenesis of atherosclerosis: atherogenesis and inflammation. *Lab. Invest.* **58**: 249–261.
- Brown, M. S., and J. L. Goldstein. 1983. Lipoprotein metabolism in the macrophage: implications for cholesterol deposition in atherosclerosis. *Annu. Rev. Biochem.* **52**: 223–261.
- Steinberg, D., S. Parthasarathy, T. E. Carew, J. C. Khoo, and J. L. Witztum. 1989. Modifications of low-density lipoprotein that increase its atherogenicity. *N. Engl. J. Med.* **320**: 915–924.
- Kilmov, A. N., A. D. Denisenko, A. V. Popov, V. A. Nagornev, V. M. Pleskov, A. G. Vinogradov, T. V. Denisenko, E. Ya. Magracheva, G. M. Kheifes, and A. S. Kuznetsov. 1985. Lipoprotein–antibody immune complexes: their catabolism and role in foam cell formation. *Atherosclerosis.* **58**: 1–15.
- Khoo, J. C., E. Miller, F. Pio, D. Steinberg, and J. L. Witztum. 1992. Monoclonal antibodies against LDL further enhance macrophage uptake of LDL aggregates. *Arterioscler. Thromb.* **12**: 1258–1266.
- Griffith, R. L., G. T. Virella, H. C. Stevenson, and M. F. Lopes-Virella. 1988. Low density lipoprotein metabolism by human macrophages activated with low density lipoprotein immune complexes. *J. Exp. Med.* **168**: 1041–1059.
- Lopes-Virella, M. F., R. L. Griffith, K. A. Shunk, and G. T. Virella. 1991. Enhanced uptake and impaired intracellular metabolism of low density lipoprotein complexed with anti-low density lipoprotein antibodies. *Arterioscler. Thromb.* **11**: 1356–1367.
- Szondy, E., M. Horvath, Z. Mezey, J. Szekely, E. Lengyel, and S. Gero. 1983. Free and complexed anti-lipoprotein antibodies in vascular diseases. *Atherosclerosis.* **49**: 69–77.
- Parums, D. V., D. L. Brown, and M. J. Mitchinson. 1990. Serum antibodies to oxidized low-density lipoprotein and ceroid in chronic periaortitis. *Arch. Pathol. Lab. Med.* **114**: 383–387.
- Beaumont, J. L., F. Doucet, P. Vivier, and M. Antonucci. 1988. Immunoglobulin-bound lipoproteins (Ig-Lp) as markers of familial hypercholesterolemia, xanthomatosis and atherosclerosis. *Atherosclerosis.* **74**: 191–201.
- Salonen, J. T., S. Ylä-Herttuala, R. Yamamoto, S. Butler, H. Korpela, R. Salonen, K. Nyyssönen, W. Palinski, and J. L. Witztum. 1992. Autoantibody against oxidized LDL and progression of carotid atherosclerosis. *The Lancet.* **339**: 883–887.
- Ylä-Herttuala, S., W. Palinski, S. W. Butler, S. Picard, D. Steinberg, and J. L. Witztum. 1994. Rabbit and human atherosclerotic lesions contain IgG that recognizes epitopes of oxidized LDL. *Arterioscler. Thromb.* **14**: 32–40.
- Fanger, M. W., L. Shen, R. F. Graziano, and P. M. Guyre. 1989. Cytotoxicity mediated by human Fc receptors for IgG. *Immunol. Today.* **10**: 92–99.
- Van de Winkel, J. G. J., and P. J. A. Capel. 1993. Human IgG Fc receptor heterogeneity: molecular aspects and clinical implications. *Immunol. Today.* **14**: 215–221.
- Guyre, P. M., R. F. Graziano, B. A. Vance, P. M. Morganelli, and M. W. Fanger. 1989. Monoclonal antibodies that bind to distinct epitopes on Fc $\gamma$ RI are able to trigger receptor function. *J. Immunol.* **143**: 1650–1655.
- Looney, R. J., G. N. Abraham, and C. L. Anderson. 1986. Human monocytes and U937 cells bear two distinct receptors for IgG. *J. Immunol.* **136**: 1641–1647.
- Fleit, H. B., S. D. Wright, and J. C. Unkeless. 1982. Human neutrophil Fc $\gamma$  receptor distribution and structure. *Proc. Natl. Acad. Sci. USA.* **79**: 3275–3382.
- Kurlander, R. J., and J. Batker. 1982. The binding of human immunoglobulin G1 monomer and small, covalently cross-linked polymers of immunoglobulin G1 to human peripheral blood monocytes and polymorphonuclear leukocytes. *J. Clin. Invest.* **69**: 1–8.
- Lubeck, M. D., Z. Steplewski, F. Baglia, M. H. Klein, K. J. Dorrington, and H. Koprowski. 1985. The interaction of murine IgG subclass proteins with human monocyte Fc receptors. *J. Immunol.* **135**: 1299–1304.
- Morganelli, P. M., T. J. Kitzmiller, R. Hemmer, and M. W. Fanger. 1992. Redirected targeting of LDL to human monocyte Fc $\gamma$  receptors with bispecific antibodies. *Arterioscler. Thromb.* **12**: 1131–1138.
- Hansson, G. K., L. Jonasson, P. S. Seifert, and S. Stemme. 1989. Immune mechanisms in atherosclerosis. *Arteriosclerosis.* **9**: 567–578.
- Fogelman, A. M., M. E. Haberland, J. Seager, M. Hokom, and P. A. Edwards. 1981. Factors regulating the activities of the low density lipoprotein receptor and the scavenger receptor on human monocyte-macrophages. *J. Lipid Res.* **22**: 1131–1141.
- Knight, B. L., and A. K. Soutar. 1982. Changes in the metabolism of modified and unmodified low-density lipoproteins during the maturation of cultured blood monocyte-macrophages from normal and homozygous familial hyper-

- cholesterolaemic subjects. *Eur. J. Biochem.* **125**: 407-413.
25. Nievelein, P. F. E. M., A. M. Fogelman, G. Mottino, and J. S. Frank. 1991. Lipid accumulation in rabbit aortic intima 2 hours after bolus infusion of low density lipoprotein. *Arterioscler. Thromb.* **11**: 1795-1805.
  26. Khoo, J. C., E. Miller, P. McLoughlin, and D. Steinberg. 1988. Enhanced macrophage uptake of low density lipoprotein after self-aggregation. *Arteriosclerosis.* **8**: 348-358.
  27. Suits, A. G., A. Chait, M. Aviram, and J. W. Heinecke. 1989. Phagocytosis of aggregated lipoprotein by macrophages: low density lipoprotein receptor-dependent foam-cell formation. *Proc. Natl. Acad. Sci. USA.* **86**: 2713-2717.
  28. Goldstein, J. L., S. K. Basu, and M. S. Brown. 1983. Receptor-mediated endocytosis of low-density lipoprotein in cultured cells. *Methods Enzymol.* **98**: 241-260.
  29. Ball, E. D., R. F. Graziano, L. Shen, and M. W. Fanger. 1982. Monoclonal antibodies to novel myeloid antigens reveal human neutrophil heterogeneity. *Proc. Natl. Acad. Sci. USA.* **79**: 5374-5378.
  30. Palinski, W., S. Ylä-Herttuala, M. E. Rosenfeld, S. W. Butler, S. A. Socher, S. Parthasarathy, L. K. Curtiss, and J. L. Witztum. 1990. Antisera and monoclonal antibodies specific for epitopes generated during oxidative modification of low density lipoprotein. *Arteriosclerosis.* **10**: 325-335.
  31. Peterson, G. L. 1977. A simplification of the protein assay method of Lowry et al. which is more generally applicable. *Anal. Biochem.* **83**: 346-356.
  32. Basu, S. K., J. L. Goldstein, R. G. W. Anderson, and M. S. Brown. 1976. Degradation of cationized low density lipoprotein and regulation of cholesterol metabolism in homozygous familial hypercholesterolemia fibroblasts. *Proc. Natl. Acad. Sci. USA.* **73**: 3178-3182.
  33. Morganelli, P. M., and P. M. Guyre. 1988. IFN- $\gamma$  plus glucocorticoids stimulate the expression of a newly identified human mononuclear phagocyte-specific antigen. *J. Immunol.* **140**: 2296-2304.
  34. Shen, L., P. M. Guyre, E. D. Ball, and M. W. Fanger. 1986. Glucocorticoid enhances gamma interferon effects on human monocyte antigen expression and ADCC. *Clin. Exp. Immunol.* **65**: 387-395.
  35. Drevon, C. A., A. D. Attie, S. H. Pangburn, and D. Steinberg. 1981. Metabolism of homologous and heterologous lipoproteins by cultured rat and human skin fibroblasts. *J. Lipid Res.* **22**: 37-46.
  36. Greenspan, P., E. P. Mayer, and S. D. Fowler. 1987. Nile Red: a selective fluorescent stain for intracellular lipid droplets. *J. Cell Biol.* **100**: 965-972.
  37. Araki, N., S. Horiuchi, A. T. M. A. Rahim, K. Takata, and Y. Morino. 1990. Microquantitation of cholesterol and cholesteryl esters in rat peritoneal macrophages by reverse-phase high performance liquid chromatography. *Anal. Biochem.* **185**: 339-345.
  38. Vercaemst, R., A. Union, and M. Rosseneu. 1989. Separation and quantitation of free cholesterol and cholesteryl esters in a macrophage cell line by high performance liquid chromatography. *J. Chromatogr.* **494**: 43-52.
  39. Bligh, E. G., and W. J. Dyer. 1959. A rapid method of total lipid extraction and purification. *Can. J. Biochem. Physiol.* **37**: 911-917.
  40. Morton, R. E., G. A. West, and H. F. Hoff. 1986. A low density lipoprotein-sized particle isolated from human atherosclerotic lesions is internalized by macrophages via a non-scavenger-receptor mechanism. *J. Lipid Res.* **27**: 1124-1134.
  41. Steinbrecher, U. P., and M. Loughheed. 1992. Scavenger receptor-independent stimulation of cholesterol esterification in macrophages by low density lipoprotein extracted from human aortic intima. *Arterioscler. Thromb.* **12**: 608-625.
  42. Shen, L., P. M. Guyre, C. L. Anderson, and M. W. Fanger. 1986. Heteroantibody-mediated cytotoxicity: antibody to the high affinity Fc receptor for IgG mediates cytotoxicity by human monocytes, which is enhanced by interferon- $\gamma$  and is not blocked by human IgG. *J. Immunol.* **137**: 3378-3382.
  43. Koolwijk, P., J. G. J. Van De Winkel, L. C. Pfefferkorn, C. W. M. Jacobs, I. Otten, G. T. Spierenburg, and B. J. E. G. Bast. 1991. Induction of intracellular Ca<sup>2+</sup> mobilization and cytotoxicity by hybrid mouse monoclonal antibodies. Fc $\gamma$ RII regulation of Fc $\gamma$ RI-triggered functions or signalling? *J. Immunol.* **147**: 595-602.
  44. Leslie, R. G. Q. 1985. Complex aggregation: a critical event in macrophage handling of soluble immune complexes. *Immunol. Today.* **6**: 183-187.
  45. Cathcart, M. K., A. K. McNally, and G. M. Chisolm. 1989. Superoxide anion participation in human monocyte-mediated oxidation of low-density lipoprotein and conversion of low-density lipoprotein to a cytotoxin. *J. Immunol.* **142**: 1963-1969.
  46. Guyre, P. M., P. M. Morganelli, and R. Miller. 1983. Recombinant immune interferon increases immunoglobulin G Fc receptors on cultured human mononuclear phagocytes. *J. Clin. Invest.* **72**: 393-397.
  47. Hoff, H. F., N. Zyromski, D. Armstrong, and J. O'Neil. 1993. Aggregation as well as chemical modification of LDL during oxidation is responsible for poor processing in macrophages. *J. Lipid Res.* **34**: 1919-1929.
  48. Heinecke, J. W., A. G. Suits, M. Aviram, and A. Chait. 1991. Phagocytosis of lipase-aggregated low density lipoprotein promotes macrophage foam cell development. *Arterioscler. Thromb.* **11**: 1643-1651.